THE MECHATRONICS AND VIBRATIONS EXPERIMENT

Technical Advisor: Daniel S. Stutts, Ph.D.

Revised: December 8, 2011

1 OBJECTIVES

1. To provide the students with a basic introduction to the concepts of electromechanical actuation and transduction, known as mechatronics.
2. To determine natural frequencies for a cantilevered beam system.
3. To estimate the damping in the cantilevered beam system
4. To determine the effect of an additional attached mass on the natural frequencies of the beam.
5. To evaluate the linearity of the system at low electric fields, and compare it to that found in high fields.

2 BACKGROUND

The use of piezoelectric actuators in ultrasonic motors, active damping of smart structures, ultrasonic welding and cutting, etc., has become widespread [1, 2, 3, 4, 5]. All of these applications combine the area of *Mechatronics*, with the theory of vibrations. Therefore, it is important to understand the basic principles in each area. Mechatronics may be defined as the combination and integration of mechanics, electronics, materials science, and electrical and control engineering. Computer science also comes in to play when higher levels of system control behavior are desired. Hence, mechatronics is a very broad and interdisciplinary field. This laboratory will touch on the materials and electrical aspects of mechatronics, and focus mostly on the mechanical aspects by developing the mathematical model of a piezoelectrically driven cantilevered beam. No development of vibration control strategies will be attempted, but may be readily undertaken as an extension if desired.

2.1 DISCLAIMER

*The author freely admits that this manual contains **WAY** too much material for the average student to absorb in the time alloted for ME242! Don't worry! You will only be tested on the material in the experimental procedure and the discussion questions. The object of including so much information in this document was to provide fertile ground for the development of extensions, and to provide the interested person with enough information to get him or her started in the field of mechatronics requiring piezoelectric actuation.*

3 SIMPLIFIED (1-D) THEORY OF PIEZOELECTRIC CERAMIC ELEMENTS

In this section, we examine the basic theory behind the thin and narrow PZT elements used to drive the cantilevered beam in this experiment. The PZT plates bonded to the aluminum beam are thin enough (14 mils or 0.356 mm) that the additional mass and stiffness contributed to the beam is negligible. In addition, since they are long and relatively narrow, we will neglect any induced strain in the y-direction perpendicular to the long axis of the beam. Hence, we need only consider the one-dimensional piezoelectric constitutive equations which pertain to the case at hand, and therefore avoid the much more complicated general case.

Before going further, we must first define the piezoelectric effect [6]:

Definition 1 *The **direct piezoelectric effect** refers the charge produced when a piezoelectric substance is subjected to a stress or strain.*

Definition 2 *The **converse piezoelectric effect** refers to the stress or strain produced when an electric field is applied to a piezoelectric substance in its poled direction.*

Hence, the direct piezoelectric effect is useful in sensors such as some microphones, accelerometers, sonar, and ultrasound transducers. The converse effect is useful in actuators such as ultrasonic welders, ultrasonic motors, and the beam in this experiment. Interestingly, both effects are employed simultaneously in sonar and ultrasound. That is, the same element which produces the sonic signal also registers the return signal.

3.1 Poling the Piezoceramic

Before PZT can be used in actuation and sensing, it must be electroded and poled. The term *poling* refers to the application of a strong electric DC field across the electrodes of the PZT. This applied *coercive* field causes most of the randomly aligned polar domains in the initially inert PZT to align with the applied field. When the field is removed, most of these realigned polar domains remain aligned in the direction of the coercive or poling field – a condition known as *remnant polarization*. The PZT is now said to be poled in the direction of the poling field, and when another electric field is applied in the same direction (+ poling direction), the PZT will expand in that direction and contract in the transverse direction. Conversely, when a field is applied in the opposite direction, the PZT will contract in the poled direction and expand in the transverse direction. This is why the piezoelectric coefficients in the transverse direction are given negative signs (see Section 10.2), and the effect is to render the transverse forcing 180 degrees out of phase with the electrical field. The situation is shown in Figure 1 where the initial (before the field is applied) size of the PZT element is indicated by dashed lines. The relevant geometry of poling is shown in Figure 2. The double arrow passing through the PZT plate indicates the positive or *down* poling direction which is in the oposite direction as the poling potential. Mathematically, the electric field is related to the potential by

$$\mathbf{E} = -\nabla \mathbf{\Phi} \tag{1}$$

where ∇ is the gradient of the applied field. By convention, the Cartesian directions x, y, and z are indicated by the numbers 1, 2, and 3 respectively. This is because in the general case, the constitutive equations are described using tensors and matrices. Also by convention, The 3-direction is always chosen to align with the positive direction of poling. The field induced in the PZT in this case is simply the applied voltage divided by the thickness of the PZT

$$E_3 = -\frac{\Phi}{h_{PZT}}. \tag{2}$$

There are numerous formulations of PZT and other piezoceramics, and each has an optimal *poling schedule*. Most manufacturers of finished piezoceramics treat the poling temperature and schedule for their ceramics as proprietary information.

3.2 The One-Dimensional Piezoelectric Constitutive Equations

Whereas the generalized Hook's law relating stress and strain is sufficient to describe the behavior of elastic materials, such as the aluminum beam in this experiment, piezoelectric materials are more complicated. In

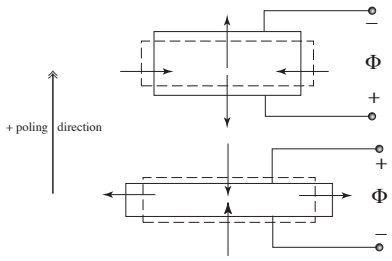

Figure 1. Strain as a function of applied field with respect to the + poling direction.

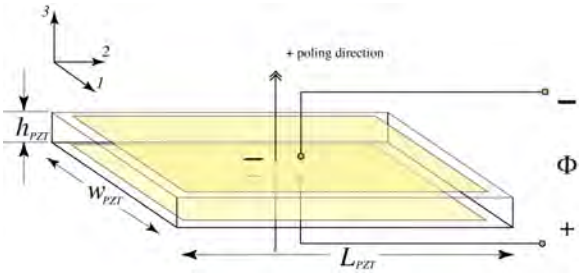

Figure 2. Schematic of relevant poling geometry.

Piezoelectric materials there is coupling between the electrical and mechanical constitutive relationships. It is, of course, this coupling which makes piezoelectric ceramics like PZT so useful. For an approximately one-dimensional piezoelectric element such as the PZT used in this experiment, the constitutive equations are given by

$$\sigma_1 = Y_{PZT}\varepsilon_1 - e_{31}E_3, \tag{3}$$

and

$$D_3 = e_{31}\varepsilon_1 + \epsilon_3 E_3, \tag{4}$$

where the parameters are defined below in Table 1. Manufacturers commonly provide the d_{31} coefficient which relates the strain in the 1-direction produced in the PZT due to an applied field in the 3-direction. The corresponding Stress relationship is given by the $e_{31} = d_{31}Y_{PZT}$ coefficient. The first subscript in this notation refers to the poled direction, and the second to the direction in which strain or stress is measured, so d_{31} is the piezoelectric coefficient relating electric field in the 3-direction to strain in the 1-direction. Equation (3) applies to the converse piezoelectric effect, and is most applicable to actuation, and Equation (4) is a statement of the direct piezoelectric effect and is most applicable to sensors[1] These two equations will be applied in both actuation and sensing later on.

Piezoelectric behavior is further complicated by the fact that the material constants are highly dependant upon the state of the material. Important variables include stress, strain, electric field, and electric displacement[2], D. This dependence may be characterized by another important piezoelectric metric: the electromechanical *coupling coefficient*. There are several frequently used definitions for the coupling coefficient, but in its basic form it is defined in one of two ways [7, 6]:

$$k^2 = \frac{\text{Electrical energy stored}}{\text{Mechanical energy input}} \tag{5}$$

[1]The permittivity of the ceramic must usually be calculated from the manufacturer's published value of the dielectric constant, $K_3 = \frac{\epsilon_3}{\epsilon_0}$, where $\epsilon_0 = 8.85 \times 10^{-12}$ Farads/m is the permittivity of free space (vacuum).

[2]D is also called the *dielectric displacement* and the *electric flux density* in the literature.

Table 1. Piezoelectric constitutive variables and constants.

Symbol	Variable Name	SI Units
σ_1	Stress in the 1-direction	Newton/ meter^2
Y_{PZT}	Young's modulus of PZT in the 1-direction	Newton/ meter^2
ε_1	Strain in the 1-direction	Dimensionless
E_3	Electric Field in the 3-direction	volt/meter
d_{31}	Strain-Form Piezoelectric constant	Coulomb/Newton or meter/volt
$e_{31} = Y_{PZT}d_{31}$	Stress-Form Piezoelectric constant	Coulomb/ meter^2 or Newton/volt-meter
D_3	Electric Displacement in the 3-direction	Coulomb/ meter^2
ϵ_3	Permittivity in the 3-direction	Farad/meter
Φ	Voltage potential in the 3-direction	Volts

or

$$k^2 = \frac{\text{Mechanical energy stored}}{\text{Electrical energy input}}. \tag{6}$$

It turns out that k is the same in either definition for a given piezoelectric. As an example, Equations (3) and (4) are more properly written

$$\sigma_1 = Y^E_{PZT}\varepsilon_1 - e_{31}E_3, \tag{7}$$

and

$$D_3 = e_{31}\varepsilon_1 + \epsilon^\varepsilon_3 E_3, \tag{8}$$

to indicate that Young's modulus is measured at constant (actually, zero) electrical field, E, and that the dielectric constant is measured at constant (zero) strain, ε. Zero field is achieved by shorting the electrodes, and zero strain is achieved by *blocking* or preventing the PZT from expanding while the field is applied. In all cases where it matters, a superscript indicates that the measurement was taken with that variable held constant, and usually zero.

For example, in the open-circuit condition, $D = 0$, and we have

$$Y^E = (1 - k^2)Y^D. \tag{9}$$

Equation (9) indicates that Young's modulus measured at constant field (short circuit) is lower than when measured at constant D (open circuit). When used as a sensor, PZT elements may be treated in the open-circuit state since the input impedance of most voltage measuring circuits is usually high. The PZT used in this experiment has coupling coefficient of $k_{31} = 0.53$, where the subscripts refer to the fact that the strain is in the 1-direction, and the induced field is in the 3-direction, so Young's modulus under the short condition is about 28% less than it is in the open circuit condition. When electrically driving the PZT in actuation, the condition is neither short nor open circuit, but there is an electric field effect as you will see during your experiments. Since the PZT is relatively thin compared to the aluminum beam, it contributes negligible stiffness, and minimal mass. The principal effect due to the variable Young's modulus is the change it causes in the e_{31} coefficient during actuation [7].

When $D = 0$, the case when PZT is used to sense strain, the strain-induced field is given by

$$E_3 = \frac{e_{31}\varepsilon_1}{\epsilon^\varepsilon_3} = \frac{-Y^D_{PZT}d_{31}\varepsilon_1}{\epsilon^\varepsilon_3}. \tag{10}$$

To obtain the voltage at a point in the PZT, the field must be integrated over the thickness of the PZT which is usually constant (h_{PZT}). Hence we have

$$\Phi = \frac{-h_{PZT} Y^D_{PZT} d_{31} \varepsilon_1}{\epsilon^{\varepsilon}_3} \tag{11}$$

However, to obtain the total voltage potential of the PZT element, the pointwise field must be integrated over the entire electroded area of the PZT element, so Equation (11) becomes

$$A_{PZT}\,\Phi = \frac{-h_{PZT} Y^D_{PZT} d_{31} \int \varepsilon_1 \, dA_{PZT}}{\epsilon^{\varepsilon}_3}, \tag{12}$$

so the total voltage induced in the PZT due to applied strain is

$$\Phi = \frac{-h_{PZT} Y^D_{PZT} d_{31}}{A_{PZT}\,\epsilon^{\varepsilon}_3} \int \varepsilon_1 \, dA_{PZT}, \tag{13}$$

where A_{PZT} is the electroded area of the PZT.

4 THE EULER-BERNOULLI BEAM MODEL

A cantilevered beam is modeled by first considering a differential element of the length dx as shown in Figure 3. This element has properties including Young's Modulus, E, area moment of inertia, I, and linear density, ρ, or mass per unit length. Assuming the presence of a distributed force per unit length, $f(x,t)$, summing forces in the y-direction (14) and summing the moments about the element (16) yields Equations (15) and (17) respectively. The higher order terms (dx^2) can be neglected in the limit as dx approaches zero. Numerous texts on the basic theory of vibrations are available which detail various aspects of beam modeling. Kelly [8], is one such example.

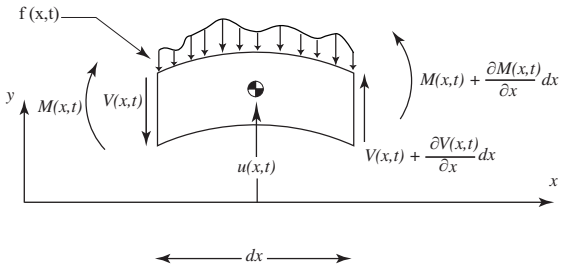

Figure 3. Differential beam element.

$$\sum F_z = \rho\, dx\, \ddot{u} = f(x,t)\, dx + V - V - \frac{\partial V}{\partial x} dx \tag{14}$$

$$\rho\, \ddot{u} + \frac{\partial V}{\partial x} = f(x,t) \tag{15}$$

$$\sum M = M + \frac{\partial M}{\partial x} dx - M - V\,\frac{dx}{2} - (V + \frac{\partial V}{\partial x} dx)\frac{dx}{2} = 0 \tag{16}$$

Equation (16) is valid under the Euler-Bernoulli assumptions of negligible mass moment of inertia and shear deformation.

$$\frac{\partial M}{\partial x} = V \tag{17}$$

It can be shown that for small slope ($\frac{\partial u}{\partial x} << 1$), that

$$M = Y_b\, I\, \frac{\partial^2 u}{\partial x^2}, \tag{18}$$

where Y_b is the Young's modulus of the beam. Substituting Equation (18) into Equation (17) and then into Equation (15) yields,

$$\rho\, \ddot{u} + \frac{\partial^2}{\partial x^2}(E\, I(x)\, \frac{\partial^2 u}{\partial x^2}) = f(x,t). \tag{19}$$

Equation (19) neglects any losses which could be modeled as velocity proportional damping. In order to solve this system we will need four boundary conditions. The boundary conditions are given by Equations (20) through (23). The boundary conditions represent zero displacement at the fixed end, zero slope at the fixed end, zero moment at the free end, and zero shear force at the free end, respectively.

$$u(0,t) = 0 \tag{20}$$

$$\frac{\partial u}{\partial x}(0,t) = 0 \tag{21}$$

$$\frac{\partial^2 u}{\partial x^2}(L,t) = 0 \tag{22}$$

$$\frac{\partial^3 u}{\partial x^3}(L,t) = 0 \tag{23}$$

4.1 Free Vibration (Unforced) Solution

Using the technique of separation of variables (SOV), a general solution with $f(x,t) = 0$ (Free Vibration) may be written as

$$u(x,t) = U(x)\, T(t). \tag{24}$$

Substitution into Equation (19) yields,

$$\rho\, U\, \frac{d^2\, T}{dt^2} = -\frac{d^2}{dx^2}(E\, I\, \frac{d^2\, U}{dx^2}\, T) \tag{25}$$

Separating the spatial and temporal components and assuming that bending stiffness, EI, is constant, yields

$$\frac{1}{T}\, \frac{d^2\, T}{dt^2} = -\frac{E\, I}{\rho\, U}\, \frac{d^4\, U}{dx^4} = -\omega^2, \tag{26}$$

where ω^2 is a constant, and will be shown to be equal to the natural frequencies of the beam. That for the left side of Equation (26) to be equal to the right hand side requires that both sides are constant stands to reason. The left side is a function of time only, and the right side is purely a function of the spatial variable, x. Hence, for Equation (26) to be valid for *all* values of t and x, requires that each side is equal to a constant. Hence, two equations result:

$$\frac{d^2\, T}{dt^2} + \omega^2 T = 0, \tag{27}$$

and

$$\frac{d^4\, U}{dx^4} - \beta^4 U = 0, \tag{28}$$

where

$$\beta^4 = \frac{\rho\,\omega^2}{E\,I}. \tag{29}$$

Equation (28) has an exponential solution of the form

$$U(x) = A\,e^{\lambda\,x}. \tag{30}$$

Substituting Equation (30) into Equation (28) yields,

$$(\lambda^4 - \beta^4)\,A\,e^{\lambda\,x} = 0, \tag{31}$$

or

$$(\lambda^2 + \beta^2)(\lambda^2 - \beta^2) = 0. \tag{32}$$

Solving for the eigenvalues (λ), yields $\lambda = \beta$, $\lambda = -\beta$, $\lambda = j\beta$, and $\lambda = -j\beta$. Hence, the general form of the spatial solution is a sum of all of the possible eigen functions, and may be written

$$U(x) = A_1\,e^{j\,\beta\,x} + A_2\,e^{-j\,\beta\,x} + A_3\,e^{\beta\,x} + A_4\,e^{-\beta\,x}. \tag{33}$$

The general solution may be rewritten in terms of trigonometric functions as

$$U(x) = B_1\,\cosh\beta\,x + B_2\,\sinh\beta\,x + B_3\,\cos\beta\,x + B_4\,\sin\beta\,x. \tag{34}$$

Applying the boundary conditions,we obtain

$$U(0) = B_1 + B_3 = 0, \tag{35}$$

$$U'(0) = \beta(B_2 + B_4) = 0, \tag{36}$$

$$U''(L) = \beta^2[B_1(\cosh\beta\,L + \cos\beta\,L) + B_2(\sinh\beta\,L + \sin\beta\,L)] = 0, \tag{37}$$

and

$$U'''(L) = \beta^3[B_1(\sinh\beta\,L - \sin\beta\,L) + B_2(\cosh\beta\,L + \cos\beta\,L)] = 0. \tag{38}$$

Combining the above yields the following equations for B_1 and B_2,

$$(\cosh\beta\,L + \cos\beta\,L)B_1 + (\sinh\beta\,L + \sin\beta\,L)B_2 = 0, \tag{39}$$

and

$$(\sinh\beta\,L - \sin\beta\,L)B_1 + (\cosh\beta\,L + \cos\beta\,L)B_2 = 0, \tag{40}$$

or in matrix form

$$\begin{bmatrix} \cosh\beta\,L + \cos\beta\,L & \sinh\beta\,L + \sin\beta\,L \\ \sinh\beta\,L - \sin\beta\,L & \cosh\beta\,L + \cos\beta\,L \end{bmatrix} \begin{pmatrix} B_1 \\ B_2 \end{pmatrix} = 0. \tag{41}$$

The determinate of the coefficient matrix in Equation (41) must vanish for nontrivial B_1 and B_2. Hence, we obtain after simplification

$$\cosh\beta\,L\,\cos\beta\,L + 1 = 0. \tag{42}$$

Equation (42) must be solved numerically for β_n where the subscript, n, denotes the fact that Equation (42) has a countable infinity of discrete roots. Table 2 gives the first four $\beta_n L_b$ values, where L_b is the length of the beam.

Table 2. First four eigenvalues multiplied by the beam length.

n	1	2	3	4
$\beta_n L_b$	1.875104	4.694091	7.854757	10.995541

Solving Equation (39) for the ratio $\frac{B_2}{B_1}$ at a given root, β_n, we have

$$(\frac{B_2}{B_1})_n = \frac{\sin\beta_n L - \sinh\beta_n L}{\cos\beta_n L + \cosh\beta_n L} \tag{43}$$

It should be noted that either (39) or (40) may be solved for this ratio, and that the resulting eigen function merely describes the shape of the individual modes, but not the amplitude of vibration. The situation here is analogous to that in finite dimensional vector spaces studied in linear algebra except that instead of discrete vectors, we have continuous functions.

From Equation (29), and recognizing the discrete nature of the eigenvalues, β_n, the natural frequencies are given by

$$\omega_n = \frac{(\beta_n L_b)^2}{L_b^2}\sqrt{\frac{E\,I}{\rho}}. \tag{44}$$

where $\rho = \overline{\rho}\,A_b$, where $\overline{\rho}$ is the mass density of the aluminum beam in kg/m^3, and A_b is the cross sectional area of the beam. The frequency in Hertz may be obtained by dividing ω_n by 2π. Thus,

$$f_n = \frac{(\beta_n L_b)^2}{2\pi L_b^2}\sqrt{\frac{E\,I}{\rho}}. \tag{45}$$

In view of Equations (35), through (38), and Equation (43), Equation (34) may be written

$$U_n(x) = \cosh\beta_n x - \cos\beta_n x + (\frac{B_2}{B_1})_n\,(\sinh\beta_n x - \sin\beta_n x)\,. \tag{46}$$

Equation (46) represents the n^{th} spatial solution, or mode shape. The corresponding temporal solution is given by

$$T_n(t) = D_1\,\cos\omega_n t + D_2\,\sin\omega_n t, \tag{47}$$

where D_1 and D_2 must be determined from the initial displacement and velocity of the beam. The total solution is thus the infinite sum of all of the modal solutions, and may be written

$$u(x,t) = \sum_{n=1}^{\infty} U_n(x)T_n(x). \tag{48}$$

4.2 The Effect of a Concentrated Mass on the Beam Natural Frequencies

The addition of a concentrated mass located at a point, $x = x^*$, on the beam has the effect of lowering some of the natural frequencies. An approximate expression for the perturbed (including the additional mass) natural frequencies may be obtained via the so-called receptance method as described in Soedel's text [9]. For the cantilevered beam, the approximate expression for the perturbed natural frequencies in Hertz is

$$f_n \approx \frac{\omega_n}{2\pi\sqrt{1+\frac{MU_n^2(x^*)}{M_b}}}, \tag{49}$$

where $U_n^2(x^*)$ is the n^{th} mode squared and evaluated at the location of the point-mass, M_b is the total mass of the beam (without the added mass), and M is the point-wise added mass. It can be seen that the attached point-mass will lower frequencies for all modes accept at those where the point of attachment corresponds to a node ($U(x^*) = 0$) which will be unchanged. For $M = 0$, we recover the original, unperturbed, natural frequency. A more accurate version of equation (49)will be given in Section 4.4.

4.3 Solution of the Damped, Moment-Forced Cantilevered Beam

Now let us consider the forced solution, where the external forcing function is not zero. In this experiment, we are forcing the beam to vibrate through the use of piezoelectric material bonded to it. The PZT forces the beam through *distributed moment forcing* [9]. As shown in Figure 5, the effective moment arm of the PZT with respect to the neutral axis of the beam is given by $r_{PZT} = \frac{h_b}{2} + \frac{h_{PZT}}{2}$. In the present case, PZT elements are bonded symmetrically to both sides of the beam, so the resulting forcing is doubled. We will neglect any external forcing perpendicular to the beam, so in this case $f(x,t) = 0$ as well, but now there is forcing due to the PZT. Again, we take the sum of the forces in the z-direction and the sum of the moments:

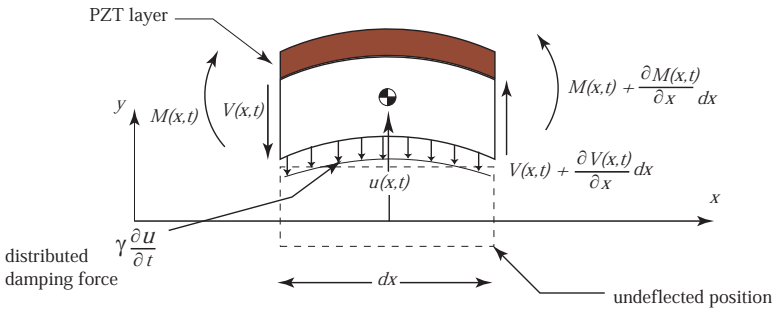

Figure 4. Differential element of a beam with PZT attached.

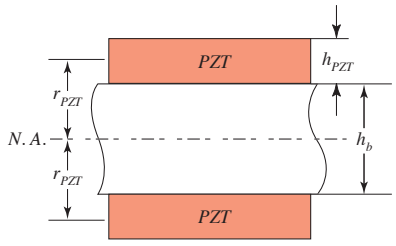

Figure 5. Schematic of PZT attachment to beam.

$$\sum F_z = \rho dx\ddot{u} = -\frac{\partial V}{\partial x}dx - \gamma\dot{u}, \tag{50}$$

where γ represents the distributed damping parameter, and has units of N-s/m^2, and

$$\sum M = \frac{\partial M}{\partial x}dx - V dx = 0. \tag{51}$$

Combining Equations (50) and (51) yields,

$$\rho\ddot{u} + \gamma\dot{u} + \frac{\partial^2 M}{\partial x^2} = 0. \tag{52}$$

The moment, $M(x,t)$, stems from two sources: mechanical stress from bending, and the converse piezoelectric effect from the PZT [10]. Neglecting the axial component of stress in the beam, i.e. assuming pure bending, the moment, M, can be defined as

$$M = b\sum_{k=1}^{n}\int_{z_k}^{z_{k+1}} z\sigma_1^k dz \tag{53}$$

where b is the width of the beam and PZT layer, z is the distance from the neutral axis, n is the total number of layers, and σ_1^k is the total stress in the layer. From Equation (3), σ_1^k can be defined as,

$$\sigma_1^k = Y_k\varepsilon_1^k - e_{31}^k E_3^k \tag{54}$$

Where Y_1^k is Young's Modulus, e_{31}^k is the converse piezoelectric constant, E_3^k is the transverse electric field, and ε_1^k is the strain in the k^{th} layer of material. Of course, not all of the possible layers are piezoelectric, and we will assume a negligible stiffness contribution from the PZT layer since it is so thin, and only located on discrete areas of the beam. The mechanical strain in the k^{th} layer is defined as

$$\varepsilon_1^k = z\frac{\partial^2 u}{\partial x^2} \tag{55}$$

where, again, z is the distance from the neutral axis of the beam. Ashton and Whitney authored a nice text on the modeling of composite structures [11].

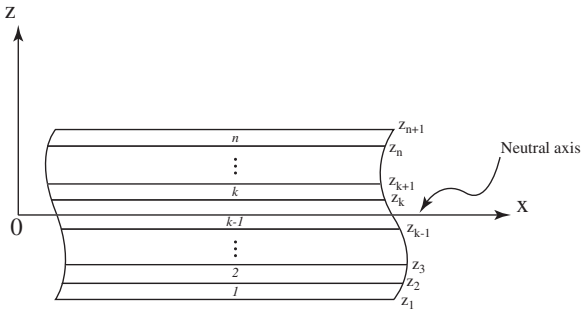

Figure 6. Schematic of lamination geometry (after Soedel [9]).

Substituting Equation (55) into (54) and then (54) into Equation (53) yields upon integration,

$$M = b\sum_{k=1}^{n}\left[Y_1^k\frac{z^3}{3}\frac{\partial^2 u}{\partial x^2} - \frac{1}{2}e_{31}^k E_3^k z^2\right]_{z_k}^{z_{k+1}}, \tag{56}$$

or

$$M = \sum_{k=1}^{n}\frac{b\,Y_1^k}{3}(z_{k+1}^3 - z_k^3)\frac{\partial^2 u}{\partial x^2} - \frac{1}{2}b\,e_{31}^k E_3^k(z_{k+1}^2 - z_k^2). \tag{57}$$

The relevant geometry is shown in Figure 6, and where in this case

$$z_1 = -(\frac{h_b}{2} + h_{PZT}) \tag{58}$$

$$z_2 = -\frac{h_b}{2} \tag{59}$$

$$z_3 = \frac{h_b}{2} \tag{60}$$

$$z_4 = \frac{h_b}{2} + h_{PZT} \tag{61}$$

The resulting moment may be expressed as a sum mechanical and electrical moments

$$M(x,t) = M^m(x,t) + M^e(x,t). \tag{62}$$

If the stiffness contribution of the PZT is neglected, mechanical and electrical moments may be shown to be

$$M^m(x,t) = \frac{1}{12} b\, h_b^3 Y_i \frac{\partial^2 u}{\partial x^2} \tag{63}$$

$$M^e(x,t) = -2\, b r_{PZT}\, d_{31}\, Y_{PZT}\, \Phi(x,t), \tag{64}$$

where we recognize the quantity $b\, h_b^3/12$ to be the area moment of inertia for a beam of rectangular cross section, usually denoted as I.

The spatially distributed voltage for a single PZT element beginning at $x = x_1$, and ending at $x = x_2$ may be expressed in terms of Heaviside step functions as

$$\Phi(x,t) = \Phi_0 \left[H(x - x_1) - H(x - x_2)\right] \sin \omega t \tag{65}$$

where Φ_0 is the amplitude of the applied voltage. The resulting voltage distribution is shown in Figure 7.

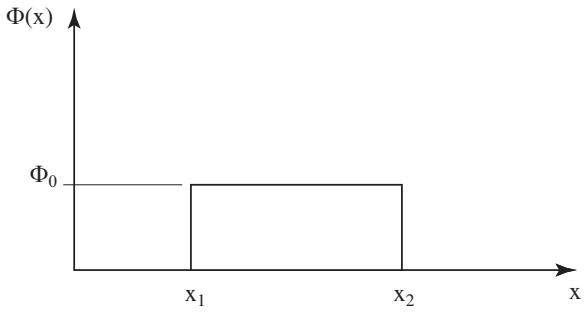

Figure 7. Voltage distribution.

Substituting the moment, M, into Equation (52) yields,

$$\rho \ddot{u} + \gamma \dot{u} + YI \frac{\partial^4 u}{\partial x^4} = 2\, b\, r_{PZT}\, d_{31}\, Y_{PZT}\, \Phi_0 \left[\delta'(x - x_1) - \delta'(x - x_2)\right] \sin \omega t, \tag{66}$$

where δ' represents the first derivative with respect to x of the Dirac delta function, which is in turn, the derivative of the Heaviside step function[3]

4.4 Modal Expansion: Orthogonality of the Natural Modes of Vibration

The concept of the orthogonality of modes represents a generalization of Fourier's series, and, having been developed by Daniel Bernoulli, actually predates Fourier's contribution [9]. In essence, the concept is analogous to the concept of orthogonal vectors in finite dimensional vector space wherein the dot (or inner) product of orthogonal vectors is zero. In function space, the inner product between two functions is defined as

$$\mathcal{I} = \int_D f\, g\, dD, \tag{67}$$

[3] Please refer to my notes on Laplace transformation which may be found at: http://www.umr.edu/~stutts/Laplace/LTHO.pdf.

where D denotes the domain over which the inner product of the functions, f, and g is defined. In general, f, and g may be functions of any number of variables. The functions f, and g are said to be orthogonal over the domain, D, if and only if

$$\int_D f\, g\, dD = 0. \tag{68}$$

The natural modes of a cantilevered beam are orthogonal, so we have

$$\int_0^{L_b} U_n(x)\, U_m(x)\, dx = \begin{cases} 0 & \text{for } m \neq n \\ N_n & \text{for } m = n \end{cases} \tag{69}$$

where $U_m(x)$, and $U_n(x)$ are any two different modes of the beam corresponding to the m^{th}, and n^{th} eigenvalues respectively, and N_n is called the *normalization factor*. The power of the orthogonality of modes will be illustrated in the following solution of Equation (66).

The more accurate version of Equation (49) to account for the change in frequency due to an attached point mass, given here now that we know about the normalization factor, is

$$f_n = \frac{\omega_n}{2\pi\sqrt{1 + \frac{M U_n^2(x^*)}{\rho N_n}}}. \tag{70}$$

As in the case of the free vibration solution, a separable solution will be assumed, but in this case, we already know the spatial solution. We will use the natural modes found in the free vibration solution. This is the so-called method of *modal expansion*. The solution may be written

$$u(x,t) = \sum_{n=1}^{\infty} U_n(x)\, \eta_n(t) \tag{71}$$

and is similar in form to that of the free-vibration solution given in Equation (48), except that the spatial solution, $U_n(x)$, is known, and the temporal solution, also known as the *modal participation factor*, $\eta_n(t)$, must be determined.

Substitution of Equation (71) into Equation (66) yields

$$\sum_{n=1}^{\infty} \left\{ \rho\ddot{\eta}(t) U_n(x) + \gamma\dot{\eta}(t) U_n(x) + YI \frac{\partial^4 U_n(x)}{\partial x^4} \eta(t) \right\} = 2\, b\, r_{PZT}\, d_{31}\, Y_{PZT}\, \Phi_0 \left[\delta'(x - x_1) - \delta'(x - x_2) \right] \sin \omega t \tag{72}$$

Recognizing from Equation (34) that

$$\frac{\partial^4 U_n(x)}{\partial x^4} = \beta_n^4 U_n(x), \tag{73}$$

we have

$$\sum_{n=1}^{\infty} \left\{ \rho\ddot{\eta}(t) + \gamma\dot{\eta}(t) + YI\beta_n^4 \eta(t) \right\} U_n(x) = -2\, b\, r_{PZT}\, d_{31}\, Y_{PZT}\, \Phi_0 \left[\delta'(x - x_1) - \delta'(x - x_2) \right] \sin \omega t. \tag{74}$$

Equation (74) may be rewritten in canonical form as

$$\sum_{n=1}^{\infty} \left\{ \ddot{\eta}_n + 2\zeta_n \omega_n \dot{\eta}_n + \omega_n^2\, \eta_n \right\} U_n(x) = F_0 \left[\delta'(x - x_1) - \delta'(x - x_2) \right] \sin \omega t, \tag{75}$$

where,

$$F_0 = \frac{2\,b\,r_{PZT}\,d_{31}\,Y_{PZT}\,\Phi_0}{\rho}, \tag{76}$$

$$\omega_n = \beta_n^2\sqrt{\frac{YI}{\rho}} = \frac{(\beta_n L_b)^2}{L_b^2}\sqrt{\frac{YI}{\rho}}, \tag{77}$$

and

$$2\zeta_n\omega_n = \frac{\gamma}{\rho}. \tag{78}$$

Equation (79) would be impossible to solve in its present form because of the infinite series on the left-hand side, so lets apply orthogonality and Equation (69) to eliminate the summation! Multiplying both sides of Equation (79) by $U_m(x)$, and integrating over the length of the beam, we have

$$\sum_{n=1}^{\infty}\left\{\ddot{\eta}_n + 2\zeta_n\omega_n\dot{\eta}_n + \omega_n^2\,\eta_n\right\}\int_0^{L_b} U_n(x)U_m(x)dx = F_0\int_0^{L_b}\left[\delta'(x-x_1) - \delta'(x-x_2)\right]U_m(x)dx\sin\omega t. \tag{79}$$

However, all of the terms in the summation vanish according to (69) except for when $m = n$ leaving:

$$\ddot{\eta}_n + 2\zeta_n\omega_n\dot{\eta}_n + \omega_n^2\,\eta_n = F_n(t), \tag{80}$$

where

$$F_n(t) = \frac{2b\,r_{PZT}d_{31}Y_{PZT}\Phi_0\left[U_n'(x_2) - U_n'(x_1)\right]}{\rho N_n}\sin\omega t. \tag{81}$$

Note that the differentiation of the Dirac delta functions has been transferred to the modes, U_n, by integration by parts. Equation (80) is an ordinary differential equation with time as an independent variable, and may be easily solved given the initial conditions of the beam. However, we are most often only interested in the steady-state solution due to the harmonic input given by Equation (81) which may be shown to be

$$\eta_n(t) = \Lambda_n\sin(\omega_n\sqrt{1-\zeta_n^2}t - \phi_n), \tag{82}$$

where,

$$\Lambda_n = \frac{F_n^*}{\omega_n^2\sqrt{(1-r_n^2)^2 + 4\zeta_n^2 r_n^2}}, \tag{83}$$

$$\phi_n = \begin{cases} \arctan\left\{\frac{2\zeta_n\omega_n}{1-r_n^2}\right\} & \text{for } r_n \le 1 \\ \pi + \arctan\left\{\frac{2\zeta_n\omega_n}{1-r_n^2}\right\} & \text{for } r_n > 1 \end{cases}, \tag{84}$$

$$F_n^* = 2\frac{br_{PZT}d_{31}Y_{PZT}V_0\left[U_n'(x_2) - U_n'(x_1)\right]}{\rho N_n}, \tag{85}$$

and $r_n = \frac{\omega}{\omega_n}$. Note also that due the fact that d_{31} will carry a negative sign, modal participation factor, $\eta_n(t)$, will lag the forcing, $F_n(t)$, by 180°.

5 EXPERIMENTAL DETERMINATION OF THE DIMENSIONLESS VISCOUS DAMPING PARAMETER

Equations (82) through (84) depend on the determination of the dimensionless damping constant, ζ_n. Fortunately, there are several ways to make this determination experimentally, and one of the most straightforward is the *logarithmic decrement* method. In this case, damping will be determined by initially

deflecting the cantilevered beam about 1cm, and releasing it to allow it to freely vibrate. Hence, we need only examine the homogeneous (unforced) case of Equation (80)

$$\ddot{\eta}_n + 2\,\zeta_n\,\omega_n\,\dot{\eta}_n + \omega_n^2\,\eta_n = 0. \tag{86}$$

In this experiment, the beam will vibrate primarily in its first mode, so the particular damping parameter we will measure is ζ_1.

A typical free response of an under damped ($\zeta < 1$) second-order system is shown in Figure 8. In this hypothetical single degree of freedom system, whose total free response is given by $x(t) = e^{-0.2t}\cos(9.998t)$, we note that there are seven peaks (labeled on the graph) before $t = 4$ seconds. This corresponds to seven complete cycles or periods of motion. As you can see from the figure, each successive peak is lower than the previous one. This decay in amplitude is governed by the indicated exponential envelope, $e^{-0.2t}$.

From our knowledge of linear systems, we know that Figure 8 represents a system where $\zeta\omega_n = 0.2$, and $\omega_d = \omega_n\sqrt{1-\zeta^2} = 9.998$, where ω_d is the so-called *damped natural frequency*. Hence, our hypothetical system has an undamped natural frequency of $\omega_n = 10$ radians per second, and a dimensionless damping parameter of $\zeta = 0.02$, or 2% of critical ($\zeta = 1$) damping.

In general, the amplitude of a second-order system at the k^{th} peak at time t_k is given by

$$x(t_k) = x_k = x_1 e^{-\zeta\omega t_k}, \tag{87}$$

where x_1 is the initial amplitude. Thus, at the first peak, $t_k = t_1 = 0$, and $x(0) = x_1$. Similarly, at the third peak,

$$x(t_3) = x_3 = x_1 e^{-\zeta\omega t_3} = x_1 e^{-\zeta\omega 2T_d}, \tag{88}$$

since there are two damped natural periods ($T_d = 2\pi/\omega_d$) between the first and third peaks. Hence, the ratio of the first peak to the k^{th} peak is given by

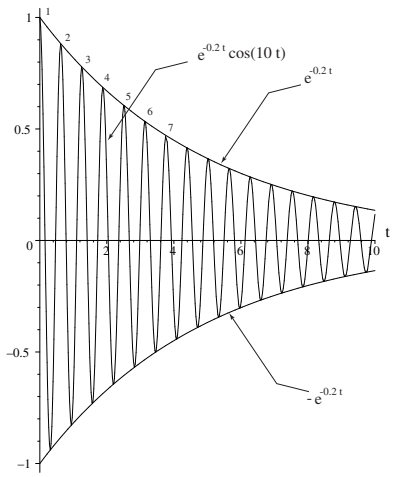

Figure 8. Typical free response of an under damped system.

$$\frac{x_1}{x_k} = e^{\zeta\omega(k-1)T_d}, \tag{89}$$

but

$$T_d = \frac{2\pi}{\omega_d} = \frac{2\pi}{\omega_n\sqrt{1-\zeta^2}}. \tag{90}$$

Hence,

$$\frac{x_1}{x_k} = e^{\zeta\omega(k-1)T_d} = e^{\frac{2(k-1)\pi}{\sqrt{1-\zeta^2}}\zeta}. \tag{91}$$

Taking the natural log of Equation (91), we obtain

$$\ln\left(\frac{x_1}{x_k}\right) = \frac{2(k-1)\pi}{\sqrt{1-\zeta^2}}\zeta = \delta_k, \tag{92}$$

where δ_k is called the *logarithmic decrement* over $k-1$ periods. It should be noted that the log ratio $\ln\left(\frac{x_i}{x_{i+1}}\right)$ is constant. In most vibrations texts, the logarithmic decrement is defined between any two adjacent peaks. We use the more general formula given in Equation (93) for this application, because the difference in amplitude between any two peaks is usually too small to accurately measure. Hence, we measure over k peaks. Solving equation (92) for ζ yields

$$\zeta = \frac{\delta_k}{\sqrt{\delta_k^2 + 4(k-1)^2\pi^2}}. \tag{93}$$

Thus, by measuring the amplitude of any two sequential peaks, and computing the logarithmic decrement, we may use Equation (93) to obtain the system dimensionless damping parameter.

Since the damped period, T_d, and ζ are known, the undamped natural frequency may be found to be

$$\omega_n = \frac{\omega_d}{\sqrt{1-\zeta^2}} = \frac{2\pi}{T_d\sqrt{1-\zeta^2}}. \tag{94}$$

For most lightly damped systems,

$$\omega_n \approx \omega_d. \tag{95}$$

REFERENCES

[1] A. Kumada U. S. Patent No. 4,868,446, Sep. 19, 1989. *Piezoelectric revolving resonator and ultrasonic motor.* 10 Claims, 17 Drawing Sheets.

[2] A. Kumada, T. Iochi and M. Okada U. S. Patent No. 5,008,581, Apr. 16, 1991. *Piezoelectric revolving resonator and single-phase ultrasonic motor.* 6 Claims, 6 Drawing Sheets.

[3] S. Ueha and Y. Tomikawa **1993** *Ultrasonic Motors—Theory and Applications.* Clarendon Press, Oxford. 297.

[4] T. Sashida U. S. Patent No. 4,562,374, Dec. 31, 1985. *Motor device utilizing ultrasonic oscillation.* 29 Claims, 22 Drawings.

[5] T. Sashida and T. Kenjo **1993** *An Introduction to Ultrasonic Motors.* Clarendon Press, Oxford. 242.

[6] B. Jaffe, W. Cook and H. Jaffe **1971** *Piezoelectric Ceramics.* Academic Press Limited, New York. 317.

[7] Takuro Ikeda **1990** *Acoustic Fields and Waves in Solids.* Oxford University Press, New York. 263.

[8] S. Graham Kelly **2000** *Fundamentals of Mechanical Vibrations.* McGraw-Hill. 629.

[9] W. Soedel **1993** *Vibrations of Shells and Plates.* Second edition. Marcel Dekker, New York. 470.

[10] H. S. Tzou **1993** *Piezoelectric Shells—Distributed Sensing and Control of Continua.* Vol. 19, Solid Mechanics and Its Applications. Kluwer, Boston. 470.

[11] J. E. Ashton and J. M. Whitney **1970** *Theory of Laminated Plates.* Technomic, Stamford, CN. 153.

[12] Ernest O. Doebelin **1990** *Measurement Systems Applications and Design.* Fourth Edition McGraw-Hill. 960.

6 EXPERIMENTAL SETUP

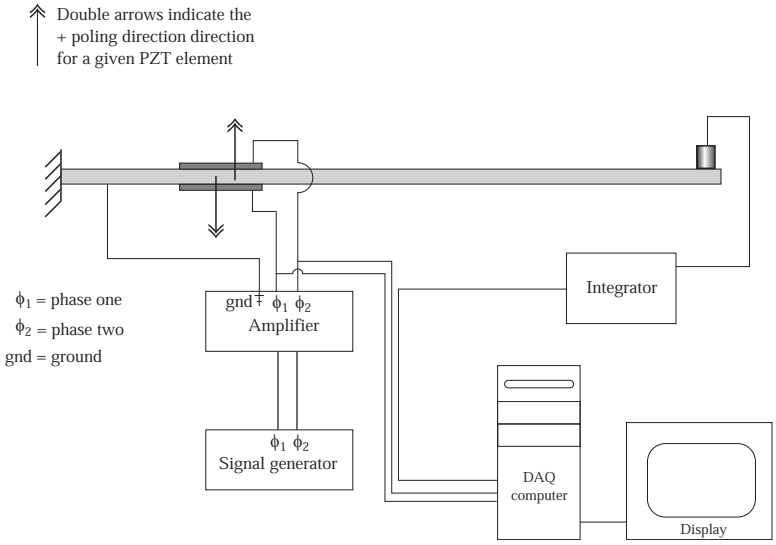

Figure 9. Schematic of experimental layout.

A schematic of the experimental layout is shown in Figure 9. The equipment consists of the following:

1. *Two-channel signal generator* – The signal generator is used to generate the sinusoidal drive signals to the power amplifier. The GTAs are familiar with the signal generator's operation and will explain the relevant controls on the front panel. The two channels may be adjusted independently. the adjustments include:
   (a) *Frequency*
   (b) *Amplitude* – the minimum amplitude is 0.05 volts, and the co-axial cables between the signal generator and the power amplifier provide a voltage limit to about 200 volts peak to peak.
   (c) *Phase* – the phase difference between the two channels may be adjusted from zero to 180 degrees.
2. *Power amplifier* – The power amplifier provides voltage amplification by a factor of 100.
3. *Accelerometer* – The accelerometer provides a voltage proportional to acceleration.
4. *Accelerometer integration unit* – Integrates the accelerometer signal twice to yield a signal proportional to position.

5. *Data acquisition lap top computer* – Provides two National Instruments Labview™ VIs (virtual instruments) to acquire the damping factor, and the steady-state amplitude. The data may be saved as tab-delimited text to a file and later imported into Excel or another spreadsheet.

6. *Aluminum beam with two PZT elements bonded to it* – The beam should be securely clamped to a solid surface before beginning the experiment. All connections to the PZT elements are independent, and may be switched around for different driving and sensing configurations. **Care should be taken not to deflect the end of the beam any more than 1 cm to avoid damaging the PZT elements.**

7. *Interconnection box* – The various inputs and outputs to and from the beam may be switched using the interconnection box. The interconnection box diagram is shown in Figure 10, and is always next to the equipment in the lab. ***Care should be taken NOT to connect the high voltage drive signal directly to the input of the data acquisition system because this will destroy the unit.*** The signal must be scaled through the interconnection box first.

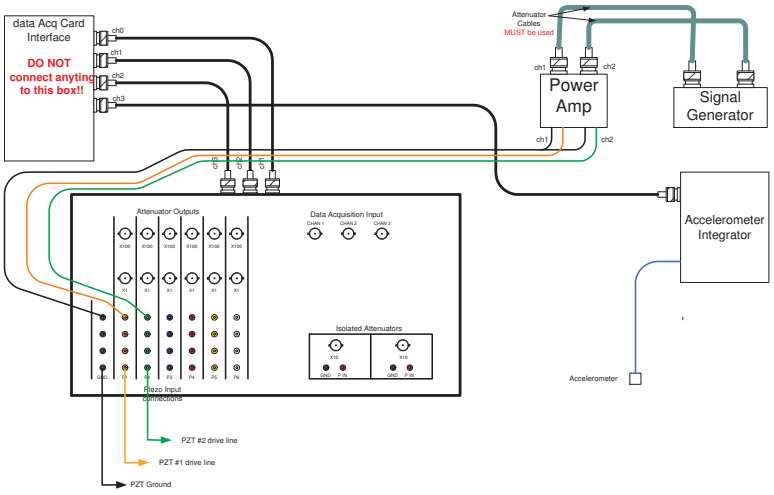

Figure 10. Interconnection box diagram.

7 DATA ACQUISITION PROCEDURE

1. Familiarize yourself with the equipment, and read *ALL* of the following instructions.

2. Measure the dimensions of the aluminum beam. Its length should be measured from the point where it is clamped to the support. Measure the distance from the base of the beam to the location of the accelerometer (x_{acc}). This will also be the location of the attached masses (x^*).

3. Make sure that the signal generator output and the power amplifier are off, and start the damping measurement VI on the computer.

4. Make sure that the integrator circuit is turned on, and the accelerometer is affixed to the end of the beam as indicated in Figure 9, then deflect the end of the beam approximately 1 cm, and release it. Press the acquire data button on the VI.

5. Position the yellow vertical line on a peak, and then the red vertical line on a subsequent peak (about 10 peaks away is best). Set the peak number including the first peak, and record the calculated value of ζ_n.

6. Determine the damped natural period, T_d, by averaging over 10 periods – i.e. the time between 11 peaks.

7. Using the sticky wax, attach a 2 gram mass to the beam just opposite to the accelerometer. Deflect the beam tip (1 cm), and repeat the damping measurement and period measurement.

8. Repeat the last step for 5 and 10 gram masses. Remove the attached mass.

9. Terminate the damping VI, and execute the steady-state measurement VI.

10. With the signal generator and power amplifier outputs off, measure the indicated peak amplitude of the accelerometer. This value represents the system bias. Take not to vibrate the beam at all during this measurement.

11. Calculate the area moment of inertia and then the first natural frequency using the $\beta_1 L_b$ value from Table 2, and Equation (44) divided by 2π to obtain the theoretical natural frequency of the first mode, f_n in Hertz.

12. Use the value of f_n to set the initial frequency of the signal generator.

13. Set the amplitude of both channels to 0.5 Volts. Make sure that one of the channels has a phase of 180 degrees, and the other channel, 0 degrees.

14. Turn on the power amplifier and the signal generator outputs, and record the indicated amplitude.

15. Set the frequency to the damped natural frequency ($f_d = 1/T_d$)(with no attached masses), and repeat the above measurement.

16. Set the amplitude of both signal generator channels to 0.05 volts, and allow the beam to settle into steady-state vibration. Select **Hold Data** and record the maximum amplitude indicated by the accelerometer. Record the peak value of the amplified voltage as well. Use the forms provided.

17. Set the amplitude to 0.1 volts, and repeat the above.

18. Repeat the above procedure in increments of 0.1 volts until you reach 0.5 volts.

19. Repeat the above procedure in descending order until you reach zero by turning off the outputs from the signal generator and power amplifier.

20. Repeat the above procedure, but this time increment from 0 to 0.05 volts, then 0.2, 0.4, 0.6, ... up to 2.6 volts indicated on the signal generator.

21. repeat the above procedure in descending order.

22. Turn off all of the equipment.

8 Experimental Analysis

The following procedures will be used to determine the full-scale and proportional errors found in the first set of amplitude versus voltage measurements done at low voltage (0 to 0.5 volts). This analysis is by no means a complete characterization of the experimental errors or the quantization errors inherent in the analog to digital conversion taking place in the data acquisition board. These errors are certainly important, but in the interest of time, we will only investigate two error metrics – full-scale and proportional error [12].

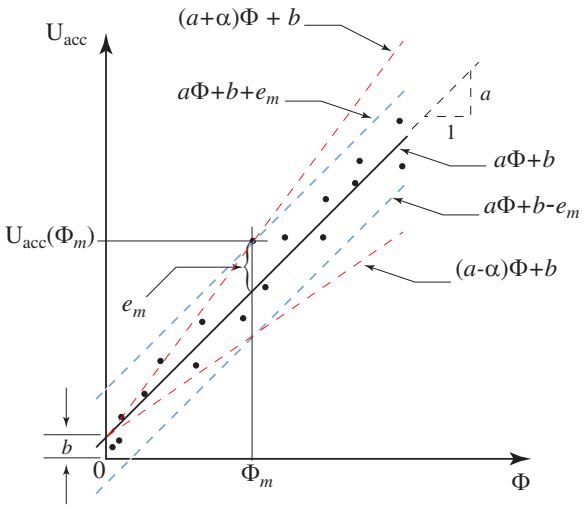

Figure 11. Least squares fit of data showing error bars.

A least squares line through a hypothetical set of data is shown in Figure 11, where U_{acc} is the displacement of the accelerometer in microns (1×10^{-6} meters), $U_m = U_{acc}(\Phi_m)$ is the value of accelerometer displacement which deviates most from the least squares line, Φ is the voltage amplitude, and Φ_m is the voltage at U_m. Also shown are the full scale error lines, and the proportional error lines which will be defined below.

Definition 3 ***Full scale error*** *is defined as the magnitude of maximum deviation from the least squares line, e_m, and is assumed to be of plus or minus constant value over the full scale. Hence, the upper and lower dotted lines parallel to the least squares line.*

The full scale error bounding curves may be computed as

$$E_{fs} = a\Phi + b \pm e_m, \tag{96}$$

where a, and b are the least squares coefficients to be defined below.

Definition 4 ***Proportional Error*** *is defined as the maximum percentage error of the measurement at the point of maximum error, and is assumed to apply to all other measurements. All other errors are assumed to occur in the same proportion to the measurement as that at the point of maximum error. Hence, the upper and lower proportional error bounding lines diverge from the least squares line, and are equal to the full scale error at the point of maximum error.*

The proportional error bounding line equations are given by

$$E_p = (a \pm \alpha)\Phi + b, \tag{97}$$

where

$$\alpha = \frac{e_m}{\Phi_m}. \tag{98}$$

Usually, both error metrics are reported, and one can assume the worst of either as a lower bound of the measurement system accuracy.

Definition 5 ***Sensitivity,*** *a, is defined as the slope of the least squares line. The least squares coefficient, a is a measure of the system measurement sensitivity.*

Definition 6 ***Bias,*** b***,*** *is defined as the intercept of the least squares line. The least squares parameter,* b *represents the system measurement bias.*

Perform the following analyses:

1. Plot the accelerometer amplitude versus the drive (amplified) voltage amplitude, and perform a least squares fit through the data to determine measurement sensitivity and bias for the low voltage range measurements (0 to 0.5 volts).
2. Determine e_m, Φ_m, and compute α, then plot the full-scale and proportional error bounding lines on the same plot as the least squares line and original data.
3. Plot the high voltage data indicating the direction (increasing or decreasing drive voltage).
4. Use Equation (49) to determine the theoretical first mode natural frequencies for each mass case – note that the accelerometer weighs 0.78 gram.
5. Compute the % error in the between the theoretical and measured natural frequencies for each mass case.
6. Compute the difference between the measured first mode natural frquencies of the beam with only the accelerometer in place as compared to that with the 10 gram mass in place.

9 DISCUSSION QUESTIONS

1. compare the measured natural frequency with the theoretical value, f_1. Why do you think these values are different if they are?
2. Using any means at your disposal, (Maple, Mathematica, MATLAB, etc.), show (at least numerically) that equation (69) is valid for modes one and two – i.e. when $n = 1$, and $m = 2$, the inner product is effectively (numerically within round off error) zero.
3. Show by integration by parts and the *filtering property* that
$$\int_a^c f(x)\delta'(x-b)dx = -f'(b) \text{ for } a < b < c, \tag{99}$$
where $\delta'(x-b)$ is the first derivative of the Dirac delta function evaluated at $x-b$.
4. How might you use Equation (13) in a practical application?
5. How was the damping constant, ζ, effected by the attached masses? Why do you suppose this is? Hint: You might examine Equations (77) and (48).

10 DATA

10.1 Beam data

$Y_b = Ys := 69 \times 10^9$ Pa (Young's modulus of the aluminum beam)
$\rho_b = 2,700$ kg/m^3 (Density of the aluminum beam)
$h_b = 0.125$ in or 0.00317 m (Thickness of the beam in the bending (z) direction)
$b = 0.5$ in or 0.0127 m (Width of the beam)
$A_b = 4.026 \times 10^{-5}$m^2 (nominal cross-sectional area of beam)
$M_{acc} = 0.78$ grams (mass of the attached accelerometer.

10.2 Piezoceramic data

$h_{PZT} = 0.000356$ m $r_{PZT} = \frac{h+tpzt}{2} = 0.001763$ m $Y_{PZT} = 71 \times 10^9$ Pa (Young's modulus)
$\rho_{PZT} = 7,700$ kg/m^3
$\epsilon_3 = 1.6 \times 10^-8$ Farad/m
$d_{31} = -171 \times 10^{-12}$ m/Volt or Coulombs/Newton

10.3 Measured data

$L_b =$ _____ (measured from clamp)

$x^* = x_{acc}$ _____ (measured from clamp)

$f_1 =$ _____ (theoretical)

$f_1 =$ _____ (measured)

$f_{1\ 2\ \text{gram}} =$ _____ (measured) _____ (Equation (49))

$f_{1\ 5\ \text{gram}} =$ _____ (measured) _____ (Equation (49))

$f_{1\ 10\ \text{gram}} =$ _____ (measured) _____ (Equation (49))

Φ_{PA} (volts)	Φ (volts)	Uacc(μm)
0.0		
0.05		
0.1		
0.15		
0.2		
0.25		
0.3		
0.35		
0.4		
0.45		
0.5		
0.45		
0.4		
0.35		
0.3		
0.25		
0.2		
0.15		
0.1		
0.05		
0.0		

Φ_{PA} (volts)	Φ (volts)	Uacc(μm)
0.0		
0.05		
0.2		
0.4		
0.6		
0.8		
1.0		
1.2		
1.4		
1.6		
1.8		
2.0		
2.2		
2.4		
2.6		
2.4		
2.2		
2.0		
1.8		
1.6		
1.4		
1.2		
1.0		
0.8		
0.6		
0.4		
0.2		
0.05		
0.0		